View metadata, citation and similar papers at core.ac.uk
brought to you by CORE
provided by CiteSeerX

Proceedings of FEDSM2007
5th Joint ASME/JSME Fluids Engineering Conference
July 30-August 2, 2007 San Diego, California USA

FEDSM2007-37442

EFFECTS OF PACKING AND ASPECT RATIO ON MIXING AND HETEROGENEOUS CATALYSIS IN MICROCHANNELS

Robert T. Bailey
Loyola College in Maryland
Baltimore, MD, USA
rtbailey@loyola.edu

Stephen Ryan
Loyola College in Maryland
Baltimore, MD, USA
smryan@loyola.edu

Frank Jones
University of Tennessee at Chattanooga
Chattanooga, TN, USA
frank-jones@utc.edu

Stephanie Wilson
University of Tennessee at Chattanooga
Chattanooga, TN, USA
siw02@yahoo.com

James Hiestand
University of Tennessee at Chattanooga
Chattanooga, TN, USA
james-hiestand@utc.edu

ABSTRACT

Many industrial chemical processes involve the mixing of two or more liquids. By reducing chemical reactors to microscale dimensions, engineers seek to take advantage of decreased diffusion lengths, leading to increased effectiveness (*e.g.*, higher purity of product) over larger process components. In this study, computational models developed using the commercial multiphysics code CFD-ACE+ are used to predict flow within microreactor channels. Two aqueous streams enter a channel—one containing a contaminant and the other devoid of the contaminant. Changes in two geometric attributes are investigated with respect to their effect on mixing of the streams: 1) packing feature layout within the channel and 2) channel aspect ratio. Reynolds numbers (*Re*) for the simulations range between 0.1 and 100. Results indicate that both packing feature position within the channel and channel aspect ratio can have a substantial impact on mixing. Between *Re* = 0.1 and *Re* = 1, mixing efficiency generally decreases with increasing *Re*; however, as the *Re* is increased from 1 to 100, fluid flow patterns in the channel are altered, and wake regions and streamline changes created by the packing features lead to improved mixing. Examples showing enhanced chemical conversion during heterogeneous catalysis as a result of better mixing are also presented.

Keywords: Mixing, Microreactor, Microchannel, Heterogeneous Catalysis, Packing, CFD Simulation

INTRODUCTION

There is currently great interest in developing microscale chemical processing devices that incorporate the inherent advantages of reduced scale [1,2]. These advantages include decreased diffusion lengths, which lead to more rapid chemical conversion rates, as well as the ability to scale processes up via simple replication. Often, such chemical devices require that two or more fluids be mixed for the desired reaction(s) to occur, and the continuous-flow, channel-based microreactor is one device that can be used for this purpose. Generally, the fluids enter at one end of the channel and mix and react as they move toward the channel exit. Because the channel cross dimensions are on the order of tens or hundreds of micrometers, the Reynolds numbers are very small (*e.g.*, less than or equal to 100), and the flow in these microreactors is laminar. Hence, the velocity fluctuations and eddies associated with turbulence are not present to help mixing occur, and mixing is restricted to molecular diffusion. The diffusion time to cross a given distance ℓ is given by [3]

$$t_D = \frac{\ell^2}{2D} \tag{1}$$

Diffusivities of many liquids are on the order of 1×10^{-9} m^2/s, which means that approximately 32 s are required to cross a 250 μm distance, while over 8 minutes are needed to travel 1 mm. Such mixing times are considered prohibitively long in some applications, so investigators have devised a number of strategies to enhance mixing and shorten mixing times. These strategies can be broadly characterized as active or passive [1,2]. Active devices utilize phenomena such acoustic, magnetic, or electrokinetic stimulation to facilitate mixing of fluids, and a power source is required. In contrast, passive devices involve no power inputs or external force fields. Instead, the geometric characteristics of the reactors are tailored to promote fluid flow patterns that enhance laminar mixing.

In the passive category, multiple channels may converge to form a concentrated mixing region where the diffusion distances are very short (*hydrodynamic focusing*) [1,2]. Alternatively, the reactor channels may include turns or bends that create vortices (*separation effects*), such as the serpentine channels investigated in [4], or they may have grooves cut into the walls to produce recirculation patterns throughout the overall flow field [5-7]. The flow streamlines exhibit folding or stretching phenomena, which form the basis for *chaotic advection* [1,2]. Micromixers may also employ a *split and recombine* strategy, where the flow stream is partitioned into many smaller

Copyright © 2007 by ASME

Downloaded From: https://proceedings.asmedigitalcollection.asme.org on 06/29/2019 Terms of Use: http://www.asme.org/about-asme/terms-of-use

streams with correspondingly reduced diffusion distances for mixing [1,2]. The separate streams mix via diffusion and are subsequently recombined to reform main flow [1,2,8,9]. Still another strategy for mixing is to place packing features within the channels [2]. These features disrupt the laminar flow structure and can lead to all four laminar mixing enhancement mechanisms listed above.

The inclusion of packing features in microchannels has been investigated experimentally by Lin *et al*. [10]. Seven vertical pillars were placed within a 50 μm-wide microchannel, perpendicular to the flow direction and in a staggered fashion. These pillars were intended to facilitate rapid mixing of two fluid streams prior to near-instantaneous freezing. Only one packing configuration was investigated, and it produced enough mixing of two reactant streams to allow for the production of some reaction intermediates in 23 μs of residence time. The short residence time was designed to capture ephemeral reaction intermediates. The same system without pillars failed to produce any of the desired reaction intermediates, presumably due to inadequate mixing of the reactant streams.

Packing features were also studied by Wang *et al*. [11], who considered eight different obstacle configurations via two-dimensional numerical simulation. The obstacles, which were circular (representing cylinders, but in two dimensions), were placed downstream of the junction of a Y-type micromixer. The channel was 300 μm wide, and the length varied from 1.2 mm to 2 mm. It was found that the obstacles improved mixing and that an asymmetric layout had more effect on the mixing than the number of obstacles.

Although the use of packing features to enhance micromixing has been studied as described above, there is a need for further systematic investigation of several parameters that can affect the quality of mixing. This computational study focuses on two such parameters—packing feature layout and channel aspect ratio—and addresses the following questions:

1. Can changes in packing feature layout significantly affect mixing efficiency within a given microchannel, and if so, what is the quantitative impact?
2. What is the quantitative impact of changes in channel aspect ratio (width to depth) for microchannels, with and without packing features.

In addition, some of the packing configurations considered in this study have also been investigated for systems involving heterogeneous catalysis, and results showing the impact of enhanced mixing on chemical conversion are also included.

THEORY AND SIMULATION APPROACH

Descriptive Equations

Flow and mixing of liquids within microchannels are described by a set of coupled nonlinear partial differential equations. For this study, several assumptions were introduced that simplify these equations:

- The two liquids being mixed are pure water and water contaminated with a relatively low concentration of a contaminant (hydrogen peroxide).
- The density and viscosity of the liquids before and after mixing are determined by the primary constituent, water. The presence of the contaminant has no appreciable effect on these parameters.
- The flow is steady and incompressible; because of the low fluid velocity and the small size of the channels, it is also laminar.
- Mixing takes place at room temperature under isothermal conditions.

With these assumptions, the flow field (velocity and pressure) within a reactor microchannel is determined by solving the following forms of the conservation of mass (continuity) and Navier-Stokes (momentum) equations:

$$\nabla \cdot \mathbf{V} = 0 \tag{2}$$

$$\rho \mathbf{V} \cdot \nabla \mathbf{V} = -\nabla p + \mu(\nabla^2 \mathbf{V}) + \rho \mathbf{g} \tag{3}$$

where $\mathbf{V}$ = Cartesian velocity vector (m/s)
ρ = bulk mixture density (kg/m^3)
p = pressure (Pa)
μ = bulk mixture absolute viscosity (N·s/m^2)
$\mathbf{g}$ = gravitational acceleration vector (m/s^2)

The steady-state concentration field is governed by

$$\mathbf{V} \cdot \nabla C - D \cdot \nabla^2 C = 0 \tag{4}$$

where C = concentration of contaminant in water (moles/L)
D = diffusivity of contaminant in water (m^2/s)

Values for the fluid flow and mass transfer parameters in the equations above are presented in Table 1.

Table 1. Flow and Mass Transfer Parameters.

Property	Value
Bulk mixture density, ρ	998 kg/m^3
Bulk mixture kinematic viscosity, $\nu=\mu/\rho$	1.31×10^{-6} m^2/s
Diffusivity of contaminant in water, D	1.0×10^{-9} m^2/s

Common Geometry and Boundary Conditions

All of the simulations presented in this paper involve two liquid streams that enter one end of a rectangular microchannel and mix to some degree as they flow axially down the channel. The channel cross sectional area varies depending on the aspect ratio being investigated, but all of the channels are 125 μm deep and 51,000 μm (51 mm) long. The two incoming streams always have equal cross sectional areas and velocities.

At the channel inlet, a uniform velocity distribution is specified for both feed streams, while at the channel exit, a fixed pressure boundary condition is assigned. A no-slip boundary condition ($\mathbf{V} = 0$) is applied at all solid surfaces. The contaminant concentration is set equal to 1000 ppm for one of the inlet streams, while the other stream is devoid of contaminant.

In cases where packing was included, the packing features are triangular prisms that span the height of the channel. This shape was selected because it divides the flow and naturally directs it laterally toward the channel side walls, where the enzyme catalyst would be present. (Other shapes could be considered, but this study held the

Copyright © 2007 by ASME

Downloaded From: https://proceedings.asmedigitalcollection.asme.org on 06/29/2019 Terms of Use: http://www.asme.org/about-asme/terms-of-use

shape constant to examine the effects of parameters other than feature shape on mixing.)

Dimensionless Parameters

Two dimensionless parameters are of particular interest in this study. The first is the mass transfer Peclet number (*Pe*), which represents the ratio of advection to diffusion mass transfer rates. This parameter is defined as

$$Pe = \frac{Ud}{D} \tag{5}$$

where U = mean velocity magnitude (m/s)
d = smallest channel cross-dimension (m)

Lower values of the Peclet number indicate situations where molecular diffusion is the dominant mechanism for mixing, while flows with higher *Pe* values reflect significant bulk transport of material in the dominant flow direction. In this study, the values of *Pe* varied between approximately 130 and 130,000.

The second dimensionless parameter of interest is the Reynolds number (*Re*), given by

$$Re = \frac{\rho U d}{\mu} \tag{6}$$

The Reynolds number represents the ratio of inertial forces to viscous forces within the moving fluid, and it is a determining factor in transition from laminar to turbulent flow. The values of *Re* in this study varied between 0.1 and 100, so all flows were laminar.

Degree of Mixing

There are several ways in which the degree of mixing at a particular axial position within the reactor channel can be quantified. Some investigators [8,12] calculate a mixing quality that is based on the ratio of the mean square deviation of the concentration field to the maximum mean square deviation at the unmixed channel entrance. Others [4] report the mixing efficiency as the ratio of the minimal and maximal concentrations over a cross section of the channel at a particular axial distance from the inlet.

If the channel is broken into two "lanes" of equal width, with the contaminated stream entering one lane (designated *A*) and the uncontaminated stream entering the other (designated *B*; see Figure 1), the mixing efficiency can also be expressed as

$$n_{mix} = 1 - \left| \frac{\overline{C}_{A,out} - \overline{C}_{in}}{\overline{C}_{A,in} - \overline{C}_{in}} \right| \tag{7}$$

Where $\overline{C}_{in}$ = average concentration of the contaminant over the entire channel inlet (moles/L)
$\overline{C}_{A,in}$ = the average concentration of the contaminant in lane *A* at the channel entrance (moles/L)
$\overline{C}_{A,out}$ = the average concentration of the contaminant in lane *A* at the channel exit (moles/L)

Equation 7, which represents the approach used in [9] and [11], has been adopted in this study.

Numerical Simulation Approach

The differential equations were solved numerically using the CFD-ACE+ computational package developed by ESI CFD, located in Huntsville, Alabama [13]. CFD-ACE+ is a finite-volume-based code that employs a variation of the SIMPLEC (Semi-Implicit Method for Pressure-Linked Equations Consistent) algorithm [14]. CFD-ACE+ has been applied previously by the authors and other investigators to simulate flow and/or reaction within microchannels [8,12,15,16]. Validation via comparison with experimental data is described in [8] and [15].

Several three-dimensional representations (models) of a single microreactor channel were created using CFD-ACE+. In each case, the channel was 125 μm deep (*y*-direction) by 51,000 μm long (*z*-direction). The channel width (*x*-direction) varied between 125 μm and 1000 μm depending on the aspect ratio. For the channels without internal features, a structured grid with approximately 225,000 cells was used. Grid points were clustered near the initial fluid interface plane and channel walls to more accurately resolve gradients there. A portion of a representative grid is shown in Fig. 1. For channels with internal features, the mesh resolution was increased to capture the more complex flow patterns, and unstructured grids consisting of around 1,000,000 cells were used. A portion of a representative grid is presented in Fig. 2. This grid resolution approached the memory limits of the available computer hardware, and sensitivity studies performed with grids of lower density indicated that further grid refinement would not lead to significant changes in the results.

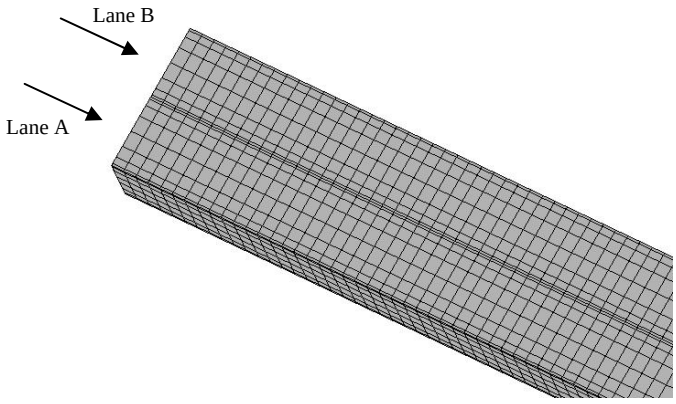

Figure 1. Portion of the Structured Grid used for the Empty Channel Cases (Lanes A and B Shown).

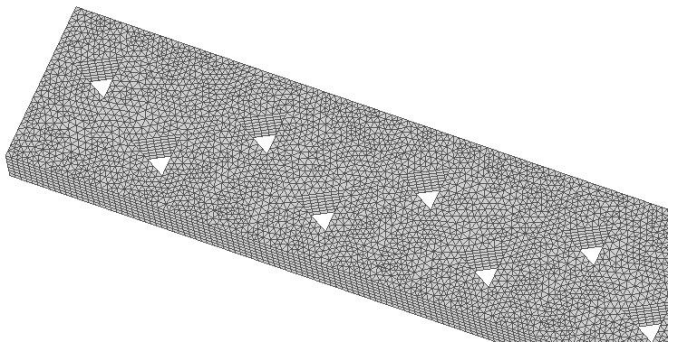

Figure 2. Portion of the Unstructured Grid used for the Cases with Packing.

Copyright © 2007 by ASME

Downloaded From: https://proceedings.asmedigitalcollection.asme.org on 06/29/2019 Terms of Use: http://www.asme.org/about-asme/terms-of-use

All computations were performed on personal computers equipped with a 3.0 or 3.6 GHz Intel Pentium 4 processors and 2 GB of RAM. The computational times ranged between 0.6 and 15.2 CPU hours depending on Reynolds number and the particular channel geometry investigated.

SIMULATION RESULTS

Effect of Feature Layout on Mixing

The first portion of this study examined the effect of packing feature layout within the channel on mixing efficiency. The channel width, depth, and length were set to 500 μm, 125 μm, and 51,000 μm (51 mm), respectively, which represents a fixed aspect ratio of 4:1. Six different packing feature cases were considered (see the first six entries in Table 2). In four of these cases, a repeating feature pattern consisting of two triangular prisms was selected, and the lateral positions of the features within the channel were varied to see how much this would affect the degree of mixing (see Cases 2A through 2D in Fig. 3). In the remaining two cases, a repeating pattern of nine triangular prisms was examined—one layout symmetric and the other asymmetric (see Cases 9A and 9B in Fig. 4). Simulations involving Reynolds numbers of 0.1, 1, 10, and 100 were run for all six cases.

Table 2. Summary of Cases Investigated.

Case	Repeating Features	Packing Feature Pattern	Aspect Ratio	Focus of Case
2A	2 triangles	in line	4:1	Effect of Packing Feature Layout on Mixing
2B	2 triangles	staggered[a]	4:1	
2C	2 triangles	staggered[a]	4:1	
2D	2 triangles	staggered[a]	4:1	
9A	9 triangles	symmetric	4:1	
9B	9 triangles	staggered	4:1	
E1	none	none	1:1	Effect of Channel Aspect Ratio on Mixing
E2	none	none	2:1	
E4	none	none	4:1	
E8	none	none	8:1	
P1	9 triangles	staggered	1:1	
P2	9 triangles	staggered	2:1	
P4	9 triangles	staggered	4:1	
P8	9 triangles	staggered	8:1	

[a] see Fig. 3 for details regarding the pattern differences between Cases 2B, 2C, and 2D

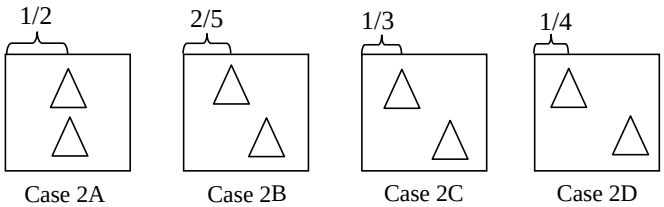

Figure 3. Two-Triangle Packing Patterns (top view of channel segment; not to scale).

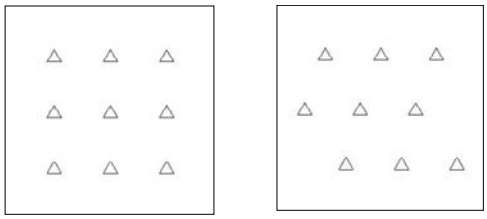

Figure 4. Nine-Triangle Packing Patterns (top view of channel segment).

A plot showing mixing efficiency as a function of Reynolds number for the four, two-triangle spacing configurations is shown in Fig. 5. (Also shown on this plot is the corresponding empty channel configuration—Case E4—as a baseline for comparison.) In general, the mixing efficiency is high (> 88 percent) in all cases at Re = 0.1—the lowest Reynolds number tested—because the lengthy residence time within the channel (45.3 s) allows significant diffusion to take place. Increasing to a Reynolds number of 1 results in a decrease in mixing, but between Re = 1 and Re = 10, the mixing efficiency begins to increase, and it rises significantly between Reynolds numbers of 10 and 100. In this range, the streamlines start to deviate substantially from simple creeping flow patterns, and laminar wake regions begin to form and grow behind the packing features. This is illustrated in Fig. 6, which shows the velocity fields along the horizontal channel mid-plane for Case 2B, Re = 10 and Re = 100. By the time Re = 100 is reached, the mixing efficiency has recovered significantly, reaching as high as 91 percent for Case 2B.

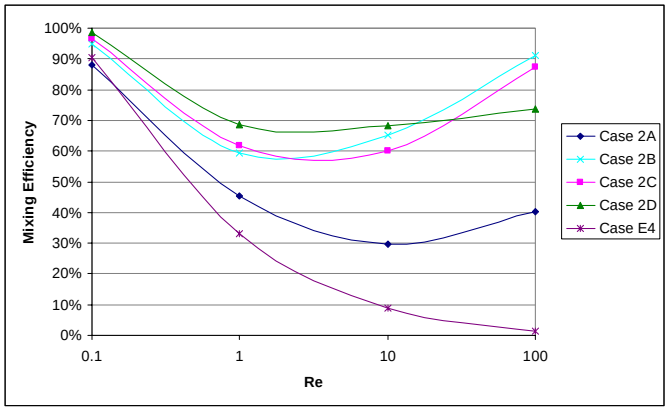

Figure 5. Results for the Two-Triangle Cases Showing the Effects of Feature Position (Empty Channel Case E4 Shown for Comparison).

It is interesting to note the variation in mixing among the cases. The packing features in each case are identical in size, shape, and number, differing only in their placement within the channel. Yet, the degree of mixing varies between 88 and 99 percent at Re = 0.1 and 40 and 91 percent at Re = 100. This indicates that feature position alone within a channel can have a significant effect on mixing, even at the low Reynolds numbers examined here. The features act to break up the flow streamlines, focusing them in some regions and creating recirculation regions in others. As anticipated, Case 2A, which places the two triangles in line with each other and

Copyright © 2007 by ASME

Downloaded From: https://proceedings.asmedigitalcollection.asme.org on 06/29/2019 Terms of Use: http://www.asme.org/about-asme/terms-of-use

does not produces significant alternating lateral fluid motion, results in less mixing than the other cases for all Reynolds numbers investigated. Among the other three cases, no one configuration is superior over all Reynolds numbers. For $Re \leq 10$, Case 2D has the highest mixing efficiency, but between $Re = 10$ and $Re = 100$, the curves for Cases 2B and 2C cross that of Case 2D. The reason for this can be seen in Fig. 7, which shows the velocity field in the horizontal mid-plane for Cases 2B and 2D at $Re = 100$. At this Reynolds number, Case 2B is the best performer, with a mixing efficiency of 91 percent. Case 2D has a corresponding efficiency of 74 percent. The velocity field for Case 2B exhibits significant lateral movement of fluid, which is very desirable in terms of fluid mixing. In contrast, the field for Case 2D shows little side-to-side activity and includes a core flow that proceeds down the center of the channel relatively undisturbed. As the Reynolds number increases, pure diffusion becomes less important, and the mixing caused by flow redistribution dominates.

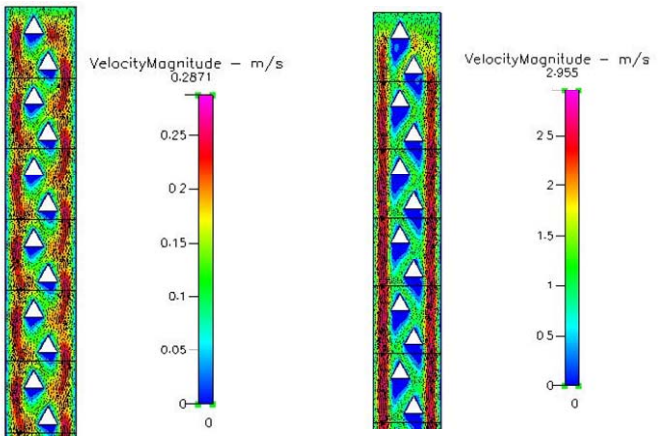

(a) $Re = 10$ (b) $Re = 100$

Figure 6. Velocity Fields along the Horizontal Channel Mid-Plane for Case 2B (top view).

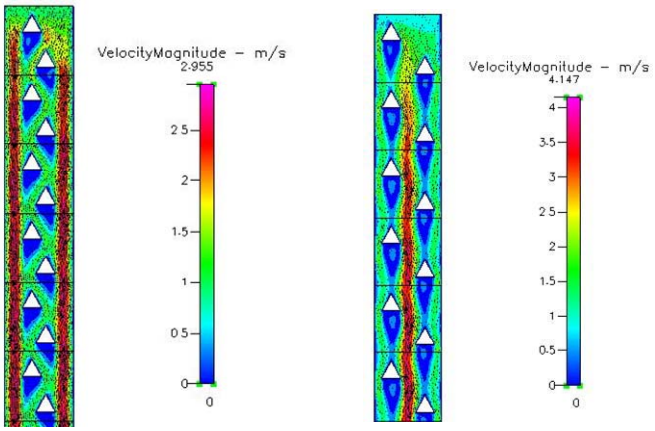

(a) Case 2B (b) Case 2D

Figure 7. Velocity Fields along the Horizontal Channel Mid-Plane for Cases 2B and 2D for $Re = 100$ (top view).

The remaining two cases involved smaller, nine-triangle patterns rather than larger, two-triangle patterns. A plot showing the mixing efficiency as a function of Reynolds number for these two cases is shown in Fig. 8. (The corresponding empty channel configuration—Case E4—is again included for comparison.) The trend of decreasing efficiency followed by increasing efficiency that was observed in Cases 2A through 2D is also present here. Also, the asymmetric layout (Case 9B) resulted in greater mixing at all Reynolds numbers examined because the asymmetry directs fluid from one side of the channel to the other in a way that the symmetric layout (Case 9A) does not (see Fig. 9). Comparing the mixing efficiencies in Figures 5 and 8, it can be seen that mixing in the asymmetric nine-feature case was less efficient than in the asymmetric two-feature cases. It is also evident that the addition of features results in a dramatic increase in mixing over the empty channel case (E4) at all but the lowest Reynolds number.

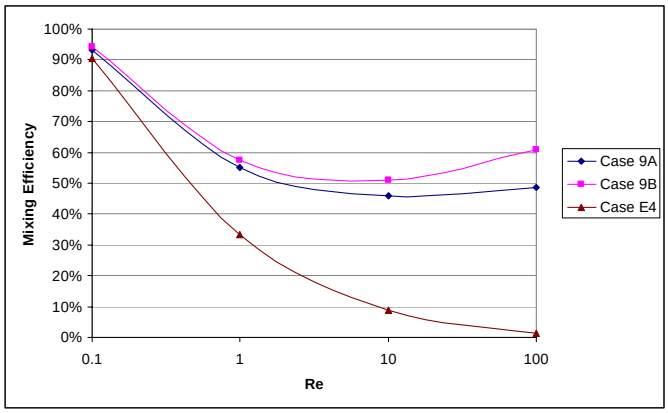

Figure 8. Results for the Nine-Triangle Cases Showing the Effects of Feature Position (Case 9A is symmetric; Case 9B is asymmetric; empty channel case E4 shown for comparison).

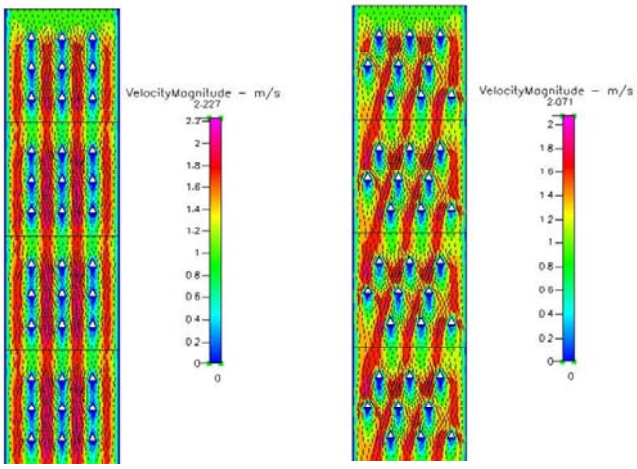

(a) Case 9A (b) Case 9B

Figure 9. Velocity Fields along the Horizontal Channel Mid-Plane for Cases 9A and 9B for $Re = 100$ (top view)

Copyright © 2007 by ASME

Downloaded From: https://proceedings.asmedigitalcollection.asme.org on 06/29/2019 Terms of Use: http://www.asme.org/about-asme/terms-of-use

Increasing the flow rate through a reactor channel also increases the pressure drop, and this must be taken into account when designing microchannel reactors for particular applications. For the two-triangle cases, the pressure drops ranged between 100 Pa and 120 Pa at *Re* = 0.1, and between 100 kPa and 270 kPa at *Re* = 100. For the nine-triangle cases, the pressure drops were between 111 Pa and 220 kPa, overall. The maximum pressure drop is still tolerable for a microchannel device in terms of structural integrity and sealing to prevent leakage [17].

Effect of Aspect Ratio on Mixing

The second part of this study focused on the impact of channel aspect ratio (width to height) on mixing. Two rectangular channel types were considered: an empty channel, and a channel with triangular-prism packing features in a nine-element, asymmetric repeating pattern (similar to Case 9B). Eight cases were examined, covering all combinations of the two channel types (empty and with features) and four aspect ratios (width:height = 1:1, 2:1, 4:1, and 8:1). As in the first portion of this study, simulations involving Reynolds numbers of 0.1, 1, 10, and 100 were run for all eight cases. These eight cases are summarized in Table 2.

Mixing efficiency results for the empty channel simulations (Cases E1, E2, E4, and E8) are shown in Fig. 10. Because there are no packing features, mixing takes place by molecular diffusion alone. It is seen from the plot that mixing efficiency decreases with increasing *Re* for all aspect ratios examined. This is as expected since the fluid residence time decreases, allowing a shorter time interval for lateral diffusion to take place. Decreasing the aspect ratio from 8:1 down to 1:1 significantly increases the mixing efficiency for all values of *Re*. For example, at *Re* = 1, the mixing efficiency increases from 16 percent to 98 percent when the aspect ratio is reduced from 8:1 down to 1:1. This was also anticipated because the diffusion travel needed for mixing is dramatically reduced as the channel becomes narrower, holding the channel depth constant at 125 μm.

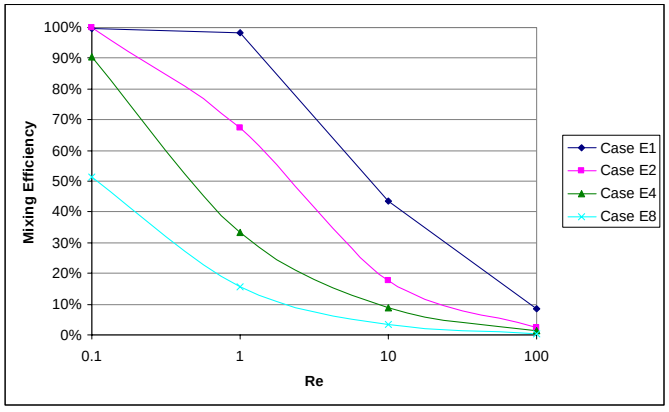

Figure 10. Results for the Empty Channel Cases Showing the Effect of Aspect Ratio

Mixing efficiency results for the packed channel simulations (Cases P1, P2, P4, and P8) are shown in Fig. 11. As with the empty channels, the mixing efficiency decreases with increasing aspect ratio, but the effect is less dramatic than in the empty channel cases. Comparing corresponding empty and packed cases at the same values of *Re* and aspect ratio, it is seen that packing always enhances mixing, but the effect becomes more pronounced as the Reynolds number increases. The behavior that was evident in the first part of this study—a decrease in mixing efficiency as *Re* increases from 0.1 to 1, followed by an increase in mixing efficiency as *Re* increases from 10 to 100—is also present in two of the cases, and for the same reason. Lateral fluid motion induced by the packing features becomes significant at higher Reynolds numbers and aspect ratios as the contribution of pure diffusion to mixing diminishes.

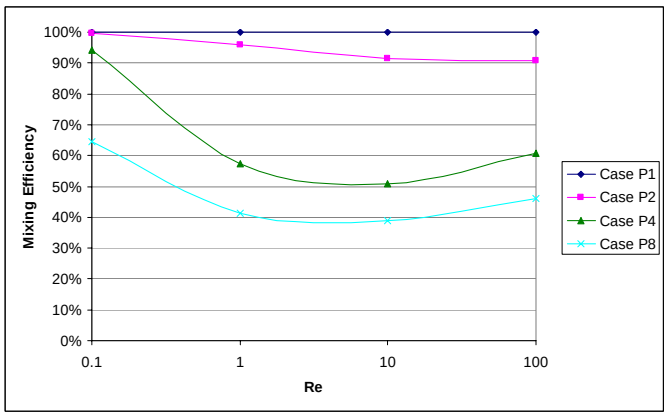

Figure 11. Results for the Nine-Triangle Cases Showing the Effect of Aspect Ratio

Although a smaller aspect ratio is always beneficial to mixing, it also results in a greater pressure drop for a fixed channel height. For the empty channel, the lowest pressure drop occurred at an aspect ratio of 8:1 and a Reynolds number of 0.1, and the value was 55 Pa. The greatest empty-channel pressure drop was 124 kPa at *Re* = 100 and an aspect ratio of 1:1. For the cases with packing, the minimum and maximum pressure drops were 73 Pa and 242 kPa, occurring at the same combinations of *Re* and aspect ratio as for the empty channel. The maximum pressure drop is again considered acceptable for a microchannel device [17].

Mixing and Heterogeneous Catalysis

Problems involving heterogeneous catalysis reactions have also been simulated for Cases 2A through 2D (two-triangle patterns) and 4E (empty channel) from Table 2. For these problems, the channel length was shortened to 10 mm, and a mixture of liquid water and 500 ppm hydrogen peroxide was introduced into the reactor across both inlet sections. The catalyst (catalase) was present on the solid surfaces of the reactor, and it facilitated the breakdown of H_2O_2 into water and dissolved oxygen at constant temperature.

A detailed discussion of these simulations is presented in [18], but a few of the results are described here in the context of enhanced mixing. Fig. 12 shows the percent conversion (destruction of H_2O_2) as a function of Reynolds number for the four, two-triangle packing cases and the corresponding empty-channel case. From this plot, it can be seen that the empty channel produces the lowest conversion percentages, indicating the benefits of including packing features. Also, no single configuration provides the highest conversion over all Reynolds numbers. As an example, a comparison of the percent conversion at *Re* = 100 is shown in Fig. 13. The presence of packing features clearly improves the percent conversion, and for these shorter channels, Case 2C is the superior performer. This is in contrast to the mixing (rather than conversion) results presented in Fig. 5, where Case 2B had the highest mixing efficiency at *Re* = 100. The difference in channel length is a possible contributing factor to

Copyright © 2007 by ASME

Downloaded From: https://proceedings.asmedigitalcollection.asme.org on 06/29/2019 Terms of Use: http://www.asme.org/about-asme/terms-of-use

this difference. However, there are other considerations associated with the behavior of flows with catalyzed chemical reaction. For homogeneous catalysis conditions, the catalyst is dispersed within the flow field, and mixing of the fluid reactants will lead in a straightforward way to higher conversion efficiencies, especially if the reaction kinetics are fast, making the process diffusion-limited. In contrast, heterogeneous catalysis, which was simulated here, is more complex. Mixing of reactants is important, but also important is the extent to which mixing promotes movement of un-reacted molecules toward the solid surfaces where the enzyme catalyst is present. There is another effect, as well. Reaction at the walls will deplete the reactants there, leading to concentration gradients and promoting molecular diffusion of reactants to the walls. All of these phenomena contribute to the resultant conversion efficiency of particular reactor configurations. In the end, however, enhanced laminar mixing is still desirable as one means to increase conversion.

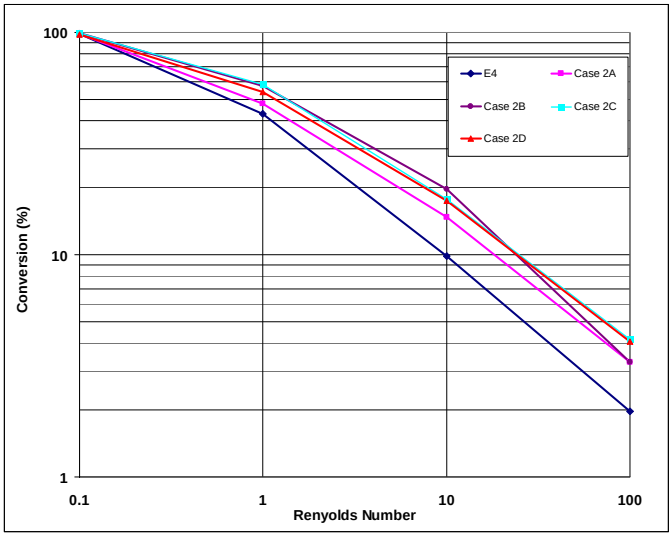

Figure 12. Heterogeneous Catalysis Results for the Two-Triangle and Empty Channel Cases Showing the Effects of Feature Position on Conversion

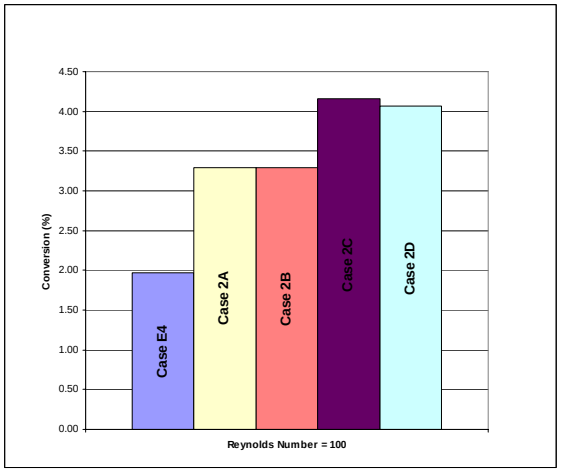

Figure 13. Comparison of the Effect of Feature Placement on Conversion at *Re* = 100.

CONCLUSIONS

The results of this study indicate that both packing feature position within the channel and channel aspect ratio can have a substantial impact on liquid mixing in straight microchannels of rectangular cross-section. Between *Re* = 0.1 and *Re* = 1, mixing efficiency generally decreases with increasing *Re*; however, as the *Re* is increased from 1 to 100, fluid flow patterns in the channel are altered by the packing features, and wake regions and streamline changes lead to improved mixing. Decreasing the aspect ratio from 8:1 down to 1:1 significantly increases the mixing efficiency for Reynolds numbers between 0.1 and 100. Mixing induced by packing features also improves chemical conversion during heterogeneous catalysis, but other factors besides fluid mixing must also be considered.

ACKNOWLEDGMENTS

The authors are grateful to the Dean of the College of Arts and Sciences at Loyola College in Maryland, who provided financial support for a portion of this work. In addition, the authors gratefully acknowledge the support of the Tennessee Center for Excellence in Applied Computational Science and Engineering via grant #R04-1302-007 (University of Tennessee at Chattanooga).

REFERENCES

[1] Hardt, S., Drese, K., Hessel, V., and Schönfeld, F., 2004, "Passive Micro Mixers for Applications in the Micro Reactor and mTAS Field," Proc. 2nd International Conference on Microchannels and Minichannels, ASME, New York, pp. 45-55.

[2] Nguyen, A., and Wu, Z., 2005, "Micromixers—a review," J. Micromech. Microeng., **15**, pp. R1-R16.

[3] Einstein, A., 1905, "On the motion of small particles suspended in liquids," Ann. Phys. (Leipz.), **17**, pp. 549-560.

[4] Mengeaud, V., J. Josserand, and H. Girault, 2002, "Mixing processes in a zigzag microchannel: finite element simulations and optical study," Anal. Chem., **74**(16), pp. 4279-4286.

[5] Stroock, A., Dertinger, S., Ajdari, A., Mezic, L., and Whitesides, G., 2002, "Chaotic mixer for microchannels," Science, 295, pp. 647-651.

[6] Stroock, A., Dertinger, S., Whitesides, G., and Ajdari, A., 2002, "Patterning flows using grooved surfaces," Anal. Chem., **74**, pp. 5306-5312.

[7] Wang, H. Iovenitti, P., Harvey, E., and Masood, S., 2003, "Numerical investigation of mixing in microchannels with patterned grooves," J. Micromech. Microeng., **13**, pp. 801-808.

[8] Lee, S. W. and Lee, S. S., 2005, "Microfabrication of the split and recombination micromixer and the effect of its cross-sectional rotation," ICMM2005-75187, Proc. 3rd International Conference on Microchannels and Minichannels, ASME, New York.

[9] Hamanaka, O. and Kato, H., 2005, "Quantitative Evaluation of Mixing Efficiency of split-and-recombine mixing method," ICMM2005-75053, Proc. 3rd International Conference on Microchannels and Minichannels, ASME, New York.

[10] Lin, Y., Gerfen, G., Rousseau, D. and Yeh, S-R., 2003, "Ultrafast microfluidic mixer and freeze-quenching device," Anal. Chem., **75**, pp. 5381-5386.

Copyright © 2007 by ASME

Downloaded From: https://proceedings.asmedigitalcollection.asme.org on 06/29/2019 Terms of Use: http://www.asme.org/about-asme/terms-of-use

[11] Wang, H., Iovenitti, P., Harvey, E., and Masood, S., 2002, "Optimizing layout of obstacles for enhanced mixing in microchannels," Smart Mater. Struct., **11,** pp. 662-667.
[12] Kockmann, N., Engler, M. Foll, C., and Woias, P., 2003, "Liquid mixing in static micro mixers with various cross sections," Proc. 1st International Conference on Microchannels and Minichannels, ASME, New York, pp. 911-918.
[13] ESI CFD Inc, 2006, "CFD-ACE+ V2006 User Manual," Huntsville, AL.
[14] Van Doormaal, J., and Raithby, G., 1984, "Enhancements of the SIMPLE method for predicting incompressible fluid flows," Numer. Heat Transfer, **7**, pp. 147-163.
[15] Bailey, R., Jones, F., Fisher, B., and Elmore, B., 2005, "Enhancing design of immobilized enzymatic microbioreactors using computational simulation," Applied Biochemistry and Biotechnology, **121-124**, pp. 639-652.
[16] Rawool, A., Sushanta, K., Mitra, K., and Kandlikar, S., 2006, "Numerical simulation of flow through microchannels with designed roughness," Microfluid. Nanofluid., **2**(3), pp. 215-221.
[17] Jones, F. Forrest, C. Palmer, J., Lu, Z., and Elmore, B., 2004, "Immobilized enzyme studies in a micro-scale bioreactor, "Applied Biochemistry and Biotechnology, **113-116**, pp. 261-272.
[18] Wilson, S., 2007, "A Study of the Effects of Various Flow Obstructions on Heterogeneous Micromixing in Biocatalytic Microchannels," Departmental Honors Thesis, University of Tennessee at Chattanooga, Chattanooga, Tennessee.

Copyright © 2007 by ASME

Downloaded From: https://proceedings.asmedigitalcollection.asme.org on 06/29/2019 Terms of Use: http://www.asme.org/about-asme/terms-of-use